Available online at www.sciencedirect.com
ScienceDirect
Bioorganic & Medicinal Chemistry 16 (2008) 3245–3254
Bioorganic & Medicinal Chemistry

Inhibition of 3(17)α-hydroxysteroid dehydrogenase (AKR1C21) by aldose reductase inhibitors

Urmi Dhagat,[a] Satoshi Endo,[b] Akira Hara[b] and Ossama El-Kabbani[a,*]

[a]*Department of Medicinal Chemistry, Victorian College of Pharmacy, Monash University, Parkville, Vic. 3052, Australia*
[b]*Laboratory of Biochemistry, Gifu Pharmaceutical University, Mitahora-higashi, Gifu 502-8585, Japan*

Received 15 October 2007; revised 10 December 2007; accepted 10 December 2007
Available online 15 December 2007

Abstract—Mouse 3(17)α-hydroxysteroid dehydrogenase (AKR1C21) is a member of the aldo-keto reductase superfamily that catalyses the oxido-reduction of steroid hormones such as estrogens, androgens and neurosteroids. Inhibitors of aldose reductase (AR), a member of the same superfamily, were evaluated against AKR1C21. Models of the enzyme–inhibitor complexes suggest that Tyr118 and Phe311 are important residues for inhibitor recognition and orientation in the active site of AKR1C21.

1. Introduction

The aldo-keto reductase (AKR) superfamily comprises NAD(P)(H)-dependent oxidoreductases that catalyse the reversible reduction of carbonyl-containing compounds to the corresponding alcohols.[1] These enzymes exhibit broad substrate specificities, with substrates ranging from alcohols and monosaccharides to steroids and prostaglandins. Proteins of the AKR superfamily possess the characteristic TIM-barrel structural motif comprising eight parallel β-sheets each associated with an α-helix that runs anti-parallel to the β-sheet.[2] Based on sequence identity, proteins of the AKR superfamily are divided into 14 families, namely AKR1 to AKR14. Within each family, proteins are further divided into sub-families based on the type of reactions they catalyse.[3] Proteins belonging to the same sub-family have 60% sequence identity but share no more than 40% sequence identity with members from other families. The largest family (AKR1) is divided into four sub-families, which include aldehyde reductases (AKR1A), aldose reductases (ARs, AKR1B), hydroxysteroid dehydrogenases (HSDs, AKR1C) and steroid 5β-reductases (AKR1D).[3,4]

Aldose reductase (EC 1.1.1.21) is the first enzyme of the polyol pathway that catalyses the reduction of glucose to sorbitol. Over-utilisation of glucose via the polyol pathway during diabetic hyperglycaemia results in intracellular accumulation of sorbitol which is implicated in the chronic complications of diabetes such as retinopathy, neuropathy and nephropathy.[5,6] Structural studies of AR have identified a wide range of potential AR inhibitors (ARIs) to combat complications arising from undesired activity of this enzyme.[7,8] Crystal structures of AR in complex with these inhibitors have revealed residues involved in inhibitor recognition and binding[9,10] and enabled implementation of successful inhibitor design strategies for the development of more selective and potent inhibitors of AR. Most inhibitors of AR can be classified into the following three groups: carboxylic acids such as tolrestat and zopolrestat, cyclic imides such as sorbinil and minalrestat and flavonoids such as quercetin and myricetin.[11–13] In spite of the rapid progress in identifying potential therapeutic compounds that would specifically bind and inhibit AR, most compounds identified to date have been unsuccessful in clinical trials due to adverse side effects.[14,15] These side effects are attributed to the inability of these compounds to selectively inhibit AR since most of these inhibitors also inhibit aldehyde reductase (AKR1A1), which also belongs to the AKR1 family.[16] AKR1A1 bears 65% sequence identity with human AR (hAR) and is involved in the reduction of diverse aldehydes to the corresponding alcohols.[17] Recent studies performed in our laboratory have shown that close similarities in the amino acid sequence and 3D structures of the two enzymes are responsible for their inhibition by the same compounds.[18,19]

Keywords: Hydroxysteroid dehydrogenases; Aldose reductase; Enzyme inhibition; Molecular modeling; Aldo-keto reductases; Drug design.
* Corresponding author. Tel.: +61 399039691; fax: +61 399039582; e-mail: ossama.el-kabbani@vcp.monash.edu.au

0968-0896/$ - see front matter © 2008 Published by Elsevier Ltd.
doi:10.1016/j.bmc.2007.12.016

Here, we report inhibition of 3(17)α-hydroxysteroid dehydrogenase (3(17)α-HSD), another member of the AKR1 family, by ARIs. 3(17)α-HSD (EC 1.1.1.209) was isolated from rabbit and mouse tissues[20–22] and has been recently identified as the 21st member of the AKR1C sub-family (AKR1C21).[22–24] Although AKR1C21 shares over 70% sequence identity with other mammalian HSDs it is unique in its ability to stereo-specifically reduce ketosteroids to the respective 17α-hydroxy derivatives. As such, AKR1C21 is the only AKR1C member known to reduce 4-androstene-3,17-dione to epitestosterone which is a 17α-epimer of testosterone that has been shown to accumulate in mammary cyst fluid and human prostate. Since mammalian HSDs regulate occupancy of steroid receptors by catalysing the oxidation-reduction reactions of the corresponding steroid hormones, they serve as important drug targets in the pre-receptor regulation of steroid hormone action.[25,26] In this study, we evaluated the inhibition of AKR1C21 by different ARIs. The three different groups of ARIs, namely, flavonoids, carboxylic acids and cyclic imides, were found to inhibit AKR1C21. Our results suggest that flavonoids are non-competitive inhibitors whereas carboxylic acids and cyclic imides are competitive inhibitors of AKR1C21. Competitive inhibitors were docked in the active site of AKR1C21 and structural comparisons were made with the ternary complexes of these inhibitors in AR. The identification of residues that may contribute to inhibitor selectivity from this study may help develop selective inhibitors of AR and 3(17)α-HSD, which are considered potential drug targets.

2. Results

2.1. Inhibition of AKR1C21 by ARIs

Compounds belonging to the three classes of ARIs, namely, flavonoids (quercetin, quercitrin, myricetin and chrysin), carboxylic acids (tolrestat and zopolrestat) and cyclic imides (sorbinil, fidarestat and minalrestat), were tested for activity against AKR1C21 (Table 1). The potency of these compounds was measured in terms of their IC_{50} values (concentration that causes 50% inhibition). Among the flavonoids, quercetin was the most potent inhibitor with an IC_{50} value of 6.9 μM followed by myricetin (IC_{50} = 12.3 μM). Quercetin-3-*O*-L-rhamnoside (quercitrin) has an IC_{50} of 33.3 μM, which makes it 4.8 times less potent than quercetin. However, in AR the inhibitory activity of quercitrin is one order of magnitude greater than that of quercetin.[27] Chrysin exhibited 36% inhibition at 12 μM concentration and was insoluble in the assay buffer above this concentration. Between the two carboxylic acid derivatives, tolrestat was more potent (IC_{50} = 48 μM) than zopolrestat (IC_{50} = 158 μM) and among the cyclic imides, sorbinil and fidarestat failed to inhibit AKR1C21 whereas minalrestat was inhibitory with an IC_{50} of 27 μM. Our results suggest that flavonoids are the most potent among the three groups of inhibitors tested. Among the carboxylic acids and the cyclic imides, minalrestat was more potent than tolrestat, which in turn was more potent than zopolrestat. The most potent inhibitors from each class were analysed further to determine their inhibition patterns. Tolrestat and minalrestat were competitive inhibitors of AKR1C21 with respect to the substrate *R*-1-indanol (K_i = 22 μM and 10.4 μM, respectively) (Fig. 1A and B). In contrast to this quercetin exhibited non-competitive inhibition with respect to the substrate *R*-1-indanol (K_i (slope effect) = 4.5 ± 0.8 μM and K_i' (intercept effect) = 11 ± 0.2 μM) (Fig. 1C). These inhibition patterns are consistent with the nature of inhibition of these compounds in AR.[27–29]

2.1.1. AKR1C21–ARI complex models. Structure–activity relationship analyses of several AR ternary complexes advocate the importance of polar groups such as carboxylates, hydroxyls and imides for potent inhibition.[30] In vitro, the carboxylic acid ARIs are potent inhibitors of AR, however, this is not translated in vivo due to their relatively low pK_a values (generally below 4) which make them ionised at physiological pH. In the ionised form, these compounds are unable to cross biological membranes and as such have poor pharmacokinetics.[31] Conversely, flavonoids and cyclic imides have better pharmacokinetic properties due to their higher pK_a values which make them neutral or partially ionised at physiological pH and can freely cross the membrane barrier.[32] Therefore, in case of AKR1C21, phenolic compounds such as the naturally occurring flavonoids are good alternatives to the carboxylic acid inhibitors. However, since quercetin showed a non-competitive inhibition pattern, its binding site in AKR1C21 will be confirmed from a crystal structure analysis as was done for the zopolrestat binding site in AR.[33] In an attempt to identify residues involved in inhibitor recognition and binding, tolrestat, zopolrestat and minalrestat were docked in the active site of AKR1C21 and these enzyme–inhibitor complex models were compared to the corresponding crystal structures of the AR ternary complexes. A comparison of the type of interaction between the inhibitors and the two enzymes was carried out to provide insights for future development of more selective and potent inhibitors against 3(17)α-HSDs.

Several crystallographic analyses and modelling studies have enabled detailed study of the inhibitor-binding site in AR.[34–37] On the contrary, the crystal structures of the AKR1C21 binary complex (with NADPH) and the AKR1C21 ternary complex (with $NADP^+$ and substrate epitestosterone) were solved very recently.[38–40] As such the ligand-binding site of AKR1C21 has not been investigated to determine molecular determinants of inhibitor binding and selectivity. Reminiscent of all members of the AKR family, both AR and AKR1C21 catalyse the reduction of a carbonyl group of substrates to a hydroxyl in an ordered bi–bi mechanism with the concomitant conversion of NADPH to $NADP^+$.[2] Both enzymes have a well-conserved 3D structure with the cofactor $NADP^+$ bound at the bottom of a deep elliptical ligand-binding site. Figure 2 shows a surface charge distribution map of the AKR1C21 molecule superimposed on the active site residues of the AR–zopolrestat complex structure. The top end of the ligand-binding pocket is formed by

Table 1. ARIs tested for inhibitory activity against AKR1C21 and their potencies shown in terms of IC_{50} values, % inhibition and no inhibition (ni) at the indicated concentrations

Compounds	Chemical structure	AKR1C21 IC_{50} (μM) or % inhibition	hAR IC_{50} (μM)
Flavonoids (phenolic derivatives)			
Quercetin	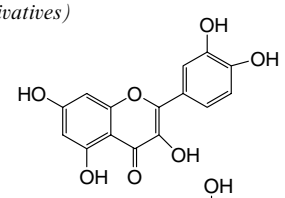	6.9 ± 0.9	2.2
Quercitrin	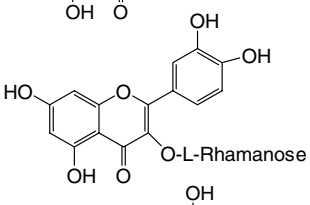	33.3 ± 10	0.15
Myricetin	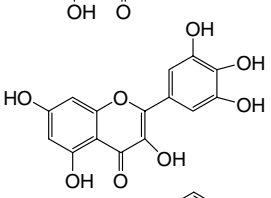	12.3 ± 2.4	29
Chrysin	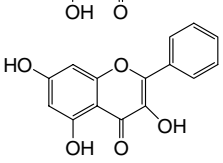	36% at 12 μM	8.5
Carboxylic acid derivatives			
Tolrestat	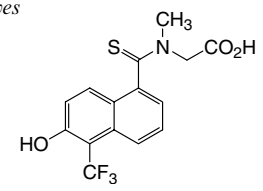	48.0 ± 4.6	0.04
Zopolrestat	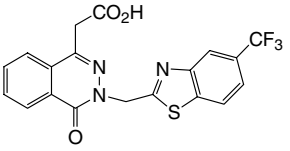	158 ± 31	0.03
Cyclic imides			
Minalrestat	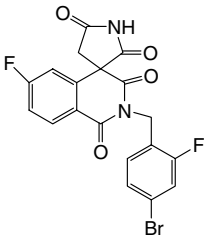	27.5 ± 3.3	0.07
Sorbinil	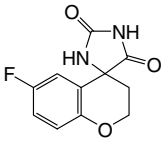	ni at 50 μM	0.91
Fidarestat	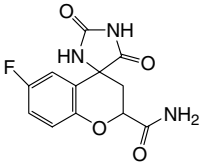	ni at 125 μM	0.009

The IC_{50} values for hAR inhibition by flavonoids,[11] carboxylic acids and cyclic imides[10,52] are also listed.

aromatic and apolar residues and the bottom comprises an anionic binding site delineated by the nicotinamide ring of the cofactor and the catalytic residues Tyr55 and His117 (Tyr48 and His110 in AR).[38,41] The special

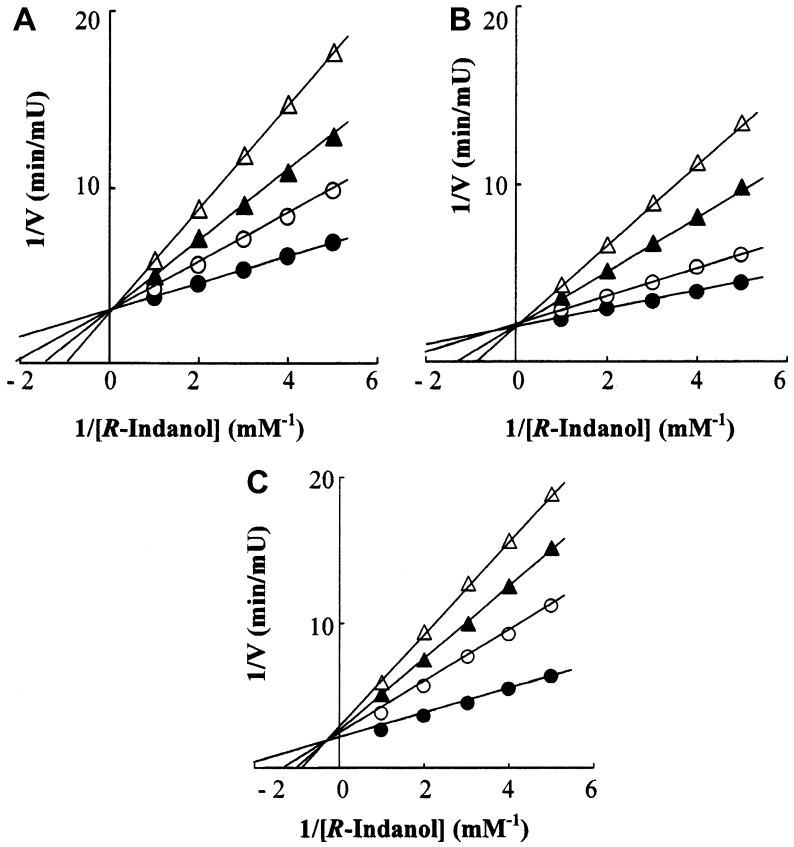

Figure 1. Inhibition patterns for AKR1C21 by tolrestat (A), minalrestat (B) and quercetin (C). The activity was determined using the five concentrations of *R*-1-indanol as the substrate in the absence (●) or presence of the inhibitor. The concentrations of tolrestat were 10 (○), 25 (▲) and 50 μM (△), those of minalrestat were 10 (○), 20 (▲) and 40 μM (△), and those of quercetin were 2 (○), 4 (▲) and 8 μM (△).

arrangement of the active site tyrosine and histidine residues and several residues lining the ligand-binding cavity that interact with the inhibitor molecules is conserved in the two enzymes. Since both enzymes have a well-conserved active site and share 63% sequence homology, the crystal structures of AR–inhibitor complexes were used as a guide for docking the inhibitors in the active site of AKR1C21 (PDB:2P5N). The enzyme–inhibitor interactions in AKR1C21 and AR models were compared to enable rational approaches to inhibitor optimisation.

2.2. Inhibitor-binding site

Potent ARIs such as tolrestat, zopolrestat and minalrestat are known to induce a conformational change upon binding in the active site of AR.[28,29] Similarly these inhibitors may induce a conformational change upon binding in the active site of AKR1C21. Since automated DOCK does not allow for such changes, these inhibitors were manually docked in the active site of AKR1C21 in an orientation similar to that in the crystal structure of corresponding AR–inhibitor complex and torsion angles of the side chains of residues coinciding with the inhibitor molecule were adjusted to avoid short contacts. Steric strain due to the docked inhibitor molecule was relieved by energy minimisation of the AKR1C21–inhibitor complex. Interactions between the docked inhibitors and the active site residues of AKR1C21 were compared to those between AR and the corresponding inhibitor in order to identify residues unique to AKR1C21 that are involved in inhibitor binding.

2.2.1. Tolrestat. Crystallographic analysis of AR in complex with tolrestat revealed that tolrestat is bound in the active site via H-bonding interactions with residues Tyr48, His110 and Trp111 (Fig. 3.1a).[28] The binding of tolrestat induces a conformational change brought about by the displacement of residues Leu300 and Phe122 of AR. This conformational change allows the hydrophobic ring system of tolrestat to bind in the 'specificity' pocket formed between residues Trp111, Leu300 and Phe122. In AR, the hydroxyl group of the naphthyl ring of tolrestat is within van der Waals contact with Phe115. The fluoride atoms of the trifluoromethyl group interface with Ser302 and Cys303 with one fluoride atom within H-bonding distance from the OH of Ser302. Tolrestat was docked in the active site of AKR1C21 using the crystal structure of AR–tolrestat ternary complex (PDB:2FZD) as a template.[42] Similar to AR, the carboxylate moiety of tolrestat was within H-bonding distance of catalytic residues Tyr55 (2.6 Å) and His117 (2.6 Å) (Fig. 3.1b). However, the H-bond between the carboxylate oxygen of tolrestat and the NE1 of Trp111 in AR is lost with the replacement of Tyr118 in place of Trp111 in AKR1C21. In AKR1C21, the hydrophobic ring system of tolrestat is sandwiched by the aromatic residues Trp227, Phe129, Trp86 and Phe311. A fluoride atom from the trifluoromethyl group

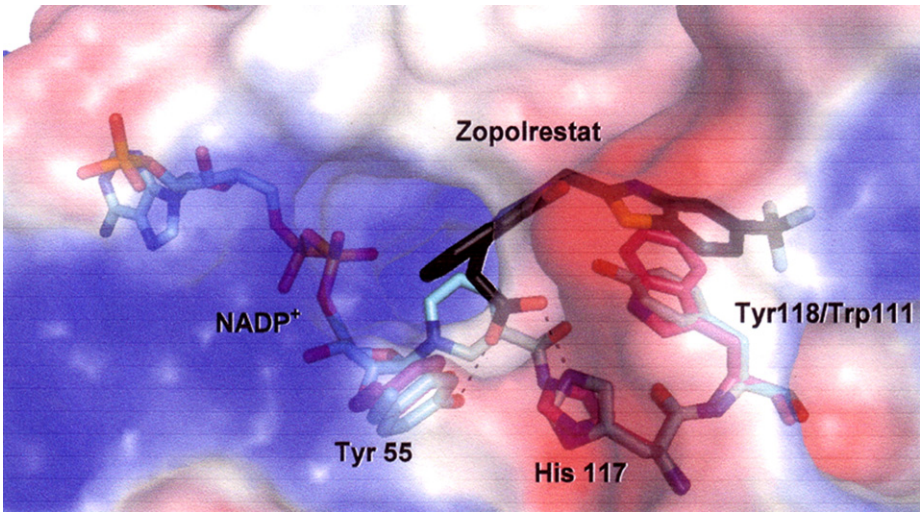

Figure 2. Surface illustration of the AKR1C21 molecule with non-polar/aromatic residues coloured in white, positively charged residues are in blue and the negatively charged residues are in red. The active site residues of hAR and AKR1C21 are superimposed and they are shown as sticks: blue (AKR1C21) and pink (AR). The inhibitor zopolrestat (black) and the cofactor (blue) are shown. H-bonding interactions between the inhibitor and catalytic residues are shown as dotted lines.

forms a H-bond with the main chain nitrogen of Phe311, which is the counterpart of Cys303 in AR.

2.2.2. Zopolrestat. Zopolrestat is bound in the active site of AR (PDB:2FZ8) with its carboxylate moiety within H-bonding distance from the residues His110, Tyr48 and Trp111 (Fig. 3.2a).[41,42] Binding of zopolrestat in AR induces a conformational change which opens the 'specificity' pocket, enabling the inhibitor to be completely sequestered in the cavity. As such, the two heterocyclic rings of zopolrestat form van der Waals contacts with residues Thr113, Leu300, Phe115, Phe122 and Trp111 of the 'specificity' pocket. The phthalazinyl ring is packed between aromatic residues Trp20 and Phe122 and benzothiazole ring π-stacks against Trp111, which is a major determinant for inhibitor binding and potency.[10] In AKR1C21, the carboxylate moiety of zopolrestat is within H-bonding distance from residues Tyr55 (2.5 Å), His117 (2.7 Å) and Tyr118 (3.0 Å) (Fig. 3.2b). The benzothiazole ring of zopolrestat makes van der Waals contacts with Phe311, Trp317, Pro318 and Met120 and π-stacks against Tyr118. The phthalazinyl ring makes van der Waals contacts with aromatic and non-polar residues Trp227, Phe129, Ala24, Val54 and Trp86.

Crystallographic analysis of the two carboxylic acid inhibitors, tolrestat[28] and zopolrestat[41] bound in the active site of AR, has enabled identification of residues involved in inhibitor recognition and binding. Both inhibitors bind in the active site with the carboxylate functional group in close proximity to C4 atom of the nicotinamide ring of the cofactor and form hydrogen bonds with Tyr48, His110 and Trp111, three key residues for inhibitor binding. Binding of these inhibitors induces a conformational change that opens the 'specificity' pocket enabling additional interactions between the enzyme and the bound inhibitors. Nevertheless, the opening of the 'specificity' pocket is different for each inhibitor depending on distinct orientation of the bound molecule. Docking of the carboxylic acid inhibitors in the active site of AKR1C21 reveals common features in the mode of binding for these inhibitors in the two enzymes. The H-bonding network between AR and these inhibitors is conserved in AKR1C21. Although Trp111 is replaced by Tyr118 in AKR1C21, it still forms H-bond and van der Waals contacts with the inhibitors. Since zopolrestat and tolrestat are orientated differently in the active site of AKR1C21 they interact with different residues in the hydrophobic cleft. The benzothiazole moiety of zopolrestat is stacked in between Tyr118 and Phe311 whereas the naphthyl ring of tolrestat is perpendicular to Tyr118. Zopolrestat, being a larger inhibitor binds much deeper in the 'specificity' pocket than tolrestat. As such, binding of zopolrestat to AKR1C21 may result in a larger energy change due to greater opening of the pocket than is the case for tolrestat, which may be responsible for more potent inhibition by tolrestat compared to zopolrestat.

2.2.3. Minalrestat. Minalrestat is bound in the active site of AR with the carbonyl oxygen atoms H-bonded to Tyr48 and Trp111 while His110 forms a hydrogen bond with the N1′ atom of the cyclic imide moiety (PDB:1PWL) (Fig. 3.3a).[29,43] In AKR1C21, minalrestat is bound in an orientation similar to that in AR however, the carbonyl oxygen atoms of the cyclic imide ring are within hydrogen bonding distances of the hydroxyl groups of Tyr55 (3.5 Å), Try118 (2.9 Å) and Tyr224 (2.6 Å), and the NE2 atom of His117 (2.7 Å). The N1′ atom of the cyclic imide moiety is within hydrogen bonding distance of the hydroxyl group of Tyr55 (3.1 Å). Minalrestat binds AR with its isoquinoline ring packed between the side chains of aromatic residues Trp20, Phe122 and Trp219.[43] In AKR1C21, the aromatic rings of minalrestat form van der Waals interactions with the surrounding aromatic residues Phe311, Trp86, Trp227 and Phe129 (Fig. 3.3b). In AR, the 4-

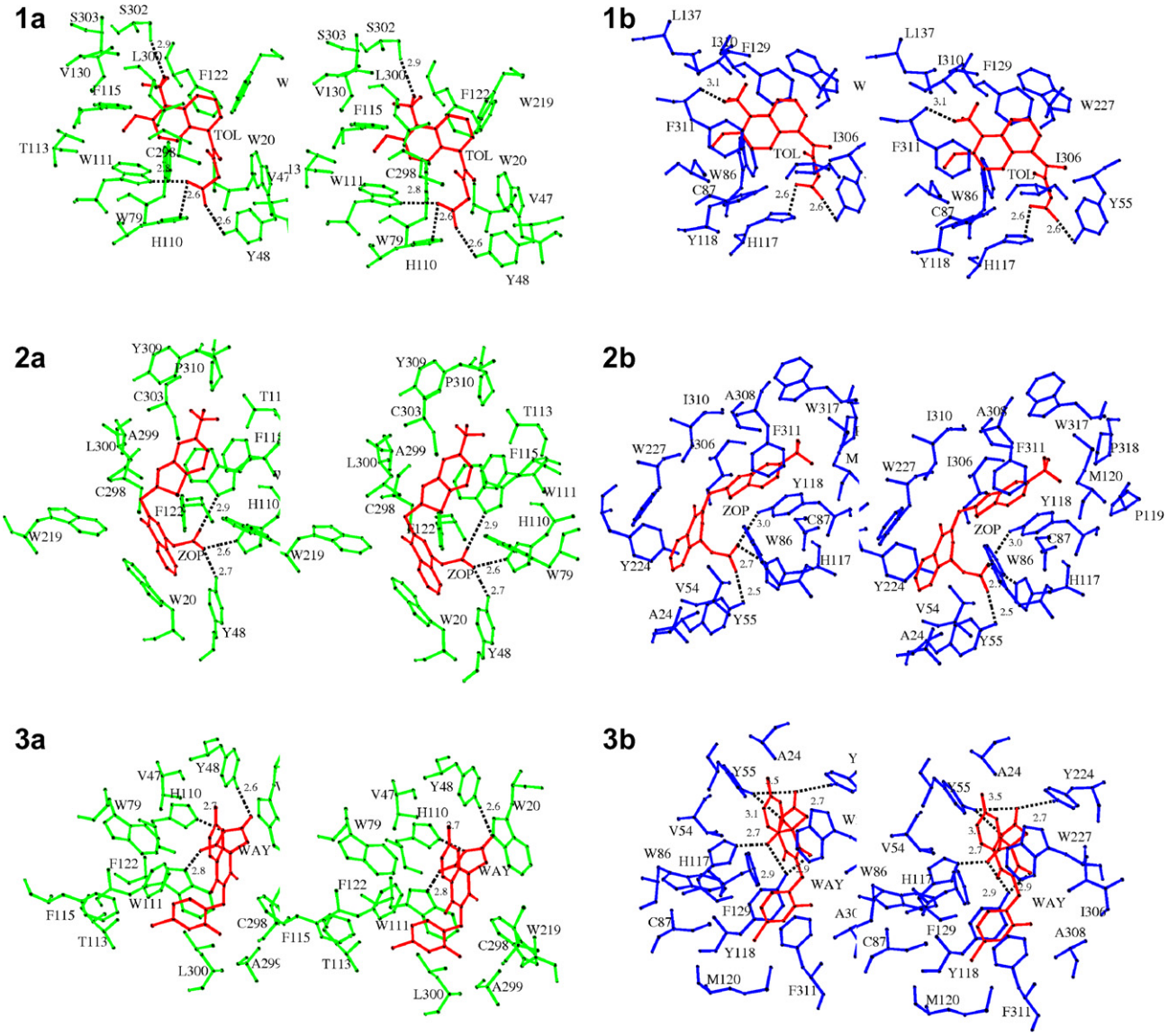

Figure 3. Stereo-view of the three inhibitors, tolrestat (1), zopolrestat (2) and minalrestat (3) bound in the active sites of hAR (a) and AKR1C21 (b). Amino acid residues within 4 Å of the inhibitor are shown and H-bond distances are given in Å.

bromo-2-fluorobenzyl group interacts with Phe122, Leu300 and Trp111 and the benzyl group π-stacks against the side chain of Trp111. The 4-bromo-2-fluorobenzyl group enters the crevice of AKR1C21 formed by residues Phe311 and Tyr118, and the benzyl group π-stacks against Phe311 and Tyr118 with the 4-bromo group present within van der Waals contacts of Cys87. The fact that minalrestat exhibits a K_i value of 10 μM whereas sorbinil and fidarestat do not inhibit AKR1C21 could be attributed to the extensive H-bonding and van

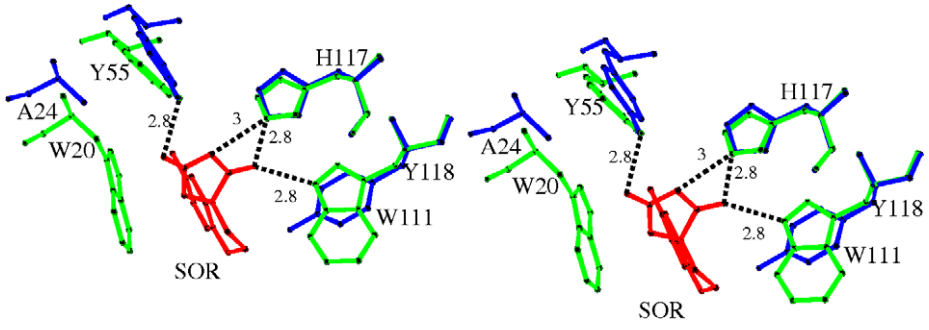

Figure 4. Superposition of the hAR and AKR1C21 inhibitor-binding sites with sorbinil modelled. The replacement of Trp20 and Trp111 interacting with the inhibitor in hAR with Ala24 and Tyr118 in AKR1C21 is likely responsible for the difference in inhibitor potency for the two enzymes.

der Waals interactions between minalrestat and AKR1C21 (Figs. 3.3b and 4). Another important point to note is that sorbinil is a relatively small inhibitor which lacks the aromatic side chain present in minalrestat that interacts with residues of the 'specificity' pocket. The presence of this additional 4-bromo-2-fluorobenzyl group in minalrestat may thus be responsible for its inhibitory activity against AKR1C21, and in turn may suggest that additional interactions between inhibitor and residues of the 'specificity' pocket in AKR1C21 are crucial for inhibition.

3. Discussion

Structural comparisons of the inhibitor-binding sites in AR and AKR1C21 reveal that the hydrogen bonding interactions between the inhibitors and active site residues Tyr55, His117 and Tyr118 (Tyr48, His110 and Trp111 in AR) are conserved (Fig. 4), and that the inhibitors are likely to be orientated in the active sites of the enzymes in a similar manner. In AR, Trp111 is involved in van der Waals contacts and H-bonding interactions with all ARIs and therefore is considered an important residue for inhibitor recognition and binding.[10] In AKR1C21, Tyr118 forms H-bonds with zopolrestat and minalrestat, and is involved in van der Waals contacts with the naphthalene ring of tolrestat. Additionally, the aromatic side chain of Tyr118 π-stacks against the benzothiazole ring and the isoquinoline ring of zopolrestat and minalrestat, respectively. As such, it is likely that Tyr118 is an important residue for inhibitor binding in the active site of AKR1C21. In AR, Trp20 is also an important residue that forms H-bonding and van der Waals interactions with the inhibitors.[10] Mutagenic analysis has revealed that the presence of an aromatic residue at this position is crucial for inhibition by sorbinil.[44] This is related to the fact that sorbinil, being a small compound, interacts mainly with the aromatic Trp20 and does not interact with the residues of the 'specificity' pocket. In AKR1C21, this aromatic residue is replaced by a much smaller residue, alanine (Ala24) (Fig. 5) which may explain why sorbinil, an inhibitor of AR fails to inhibit AKR1C21.

The three ARIs discussed in this study induce a conformational change which opens the 'specificity' pocket of AR enabling the inhibitors to bind to the active site. In AR, the 'specificity' pocket comprises residues Thr113, Phe115, Phe122, Val130, Leu300, Ser302 and Cys303.[28] Inhibitors that form van der Waals contacts with these residues tend to be more selective for AR

Figure 5. The amino acid sequences of AKR1C21 and hAR were aligned using the program CLUSTALW (version 1.83) with default values for all parameters, introducing as few insertions (shown by hyphens) as possible to conserve conformational aspects of the molecules. Identical residues are represented by '*', highly conserved residues as ':', weakly conserved substitutions are represented by '.' and the unmarked residues are non-conserved. Catalytic residues of the enzymes are shaded in green and residues interacting with the inhibitors are shaded in grey, respectively.

relative to other family members such as aldehyde reductase. The difference in potency of these inhibitors for the two enzymes is attributed to differences in the residues of the C-terminal loop that partly form the 'specificity' pocket.[45,46] In this study, we have identified residues Ile306, Ala308, Ile310, Phe311, Trp317 and Pro318 (Fig. 5) of the C-terminal loop of AKR1C21 that are involved in van der Waals interactions with the three modelled ARIs. Out of these, Ile306, Ala308, Ile310 and Phe311 are non-conserved between AR and AKR1C21 and could be responsible for the differences in the potency of these inhibitors for the two enzymes. Of particular importance is Phe311, which forms van der Waals contacts with the heterocyclic rings of tolrestat and π-stacks against the benzothiazole ring and the isoquinoline ring of zopolrestat and minalrestat, respectively. Its main chain nitrogen atom forms a H-bond with a fluoride atom from tolrestat. Based on these observations, it is possible that Phe311 plays an important role in inhibitor binding and selectivity, a role similar to that reported for Leu300 in AR.[19]

Moreover, the extent of the conformational change that is induced upon binding of inhibitors to AR may vary in AKR1C21, which may partly account for the difference in inhibitor potency between the two enzymes, as reflected in the IC_{50} values listed in Table 1. It is possible that the flavonoids induce little or no conformational change since they have relatively similar IC_{50} values for both enzymes whereas zopolrestat, tolrestat and minalrestat that induce a conformational change upon binding to AR show considerably less potency against AKR1C21. While these compounds are less potent against AKR1C21 compared to AR, they may be useful as a starting point for the development of selective and more potent inhibitors of 3(17)α-HSDs.

Molecular modelling and kinetic analysis of ARIs against AKR1C21 confirm two important structural features necessary for the inhibition of the AKRs.[19] The first being the presence of a charged group such as the carboxylate moiety in tolrestat, the phenol group in quercetin or the cyclic imide moiety in minalrestat. These charged groups are important for electrostatic interactions with the positively charged nicotinamide ring of the cofactor and with the active site residues. The second important feature is the presence of a hydrophobic ring system that is involved in π-stacking and van der Waals interactions with the non-polar and aromatic residues of the binding pocket. In AR, interactions between the aromatic side chains of the inhibitors and the hydrophobic residues of the 'specificity' pocket are crucial for inhibitor potency and selectivity.[30,47] Similarly in AKR1C21, the hydrophobic residues lining the ligand-binding cavity that interact with the aromatic side chains of these inhibitors would serve as important determinants for inhibitor binding and potency. However, the exact role of these residues in inhibitor binding has yet to be confirmed by site-directed mutagenesis. These structural features may form an important basis for future design of selective inhibitors for 3(17)α-HSDs.

4. Conclusion

Molecular modelling and kinetic studies identified new inhibitors against AKR1C21 with competitive and non-competitive inhibition patterns. The inhibitors possess a core template that utilises H-bonding and van der Waals interactions with the enzyme to position the polar head of the inhibitor to interact with the catalytic residues His117 and Tyr55 of AKR1C21. Phe311 and Tyr118 are important determinants for inhibitor recognition and binding in AKR1C21 and mutagenic analysis of these residues (Tyr118 and Phe311) would help confirm their exact role in inhibitor recognition and selectivity. Additionally, it will be important to determine the crystal structure of AKR1C21 in complex with inhibitor in order to confirm the interaction with key amino acid residues and their role in achieving the optimal inhibitor binding conformation. Knowledge of the type of interactions between the enzyme and inhibitor can be used to design compounds that are tailored to selectively bind and inhibit 3(17)α-HSDs.

5. Experimental

5.1. Enzyme kinetics

Recombinant AKR1C21 was expressed and purified to homogeneity as described previously.[22,23] The dehydrogenase activity of the enzyme was determined at 25 °C by monitoring the rate of formation of NADPH at 455 nm with an excitation wavelength of 340 nm. The reaction mixture consisted of 0.1 M potassium phosphate, pH 7.4, 0.25 mM $NADP^+$, 1 mM *R*-1-indanol (Fluka) and enzyme in a total volume of 2.0 ml. One unit (**U**) of enzyme activity was defined as the amount that catalyses the formation of 1 μmol of NADPH per min. All inhibitors were dissolved in methanol, except for zopolrestat and chrysin that were insoluble in methanol and were dissolved in a 1:1 mixture of dimethylsulfoxide and methanol stock solution. The stock solution was diluted further with methanol and 25 μl of this was added to the reaction mixture. The final concentration of methanol in the reaction mixture was less than 2%. Initially, the IC_{50} values for the inhibitors were determined and then their inhibition patterns and K_i values were analysed using five concentrations of the substrate by the Lineweaver–Burk plot, Dixon plot and/or Cornish–Bowden plot[51] of the velocities obtained with four concentrations of the inhibitor. The IC_{50} and K_i values are expressed as means ± standard deviation of three determinations.

5.2. Molecular modelling

Based on the high sequence similarity (63%) and a well-conserved active site the crystal structures of the AR ternary complexes were used as templates for docking respective inhibitors in the active site of AKR1C21 (PDB:2P5N). The structural coordinates of the hAR ternary complexes were obtained from the RCSB protein data bank (http://www.rcsb.org). Among the several AR structures available, 2FZD was used for docking

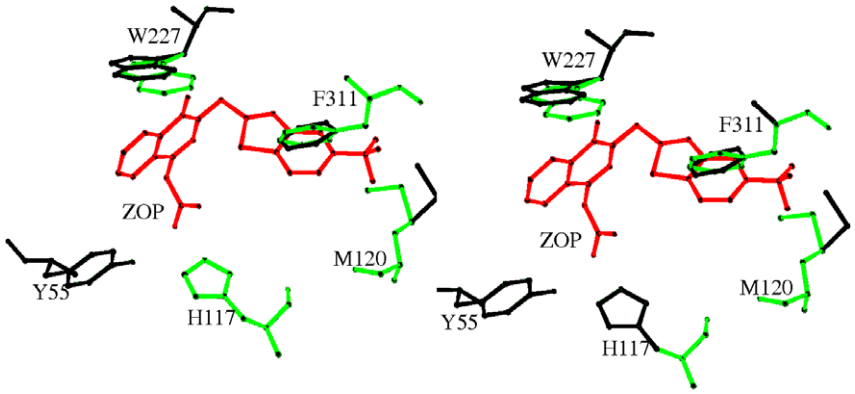

Figure 6. Superposition of the AKR1C21 inhibitor-binding site before and after docking zopolrestat. The manual changes in the side chains of Met120, Trp227 and Phe311 to accommodate the inhibitor are shown.

tolrestat, 2FZ8 was used for zopolrestat and 1PWL was used for minalrestat. All ARIs used in the modelling study are known to induce a conformational change upon binding in the active site, especially in the flexible C-terminal loop. Since automated DOCK does not allow for any such changes, these inhibitors were manually docked in the active site of AKR1C21 after the two enzymes were superimposed in InsightII. The inhibitors were docked in an orientation similar to that of the crystal structure of the corresponding AR–inhibitor complex. The polar heads of the inhibitor molecules were placed within hydrogen bonding distance of the catalytic residues Tyr55 and His117. Since carboxylic acids have a relatively low pK_a value which makes them ionised at physiological pH, the hydrophilic head (COOH) was bound in the COO^- form, with the negative charge shared between oxygen atoms of the carboxylic moiety. The cofactor used in the docking studies was $NADP^+$. Hydrogen atoms, partial charges, atomic potentials and bond orders were assigned to the protein–inhibitor complexes using the automatic procedures within the InsightII 2.1 package (Biosym Technologies Inc., San Diego, CA). Any clashes between the newly docked inhibitor molecules and the side chains of the residues of the binding pocket were removed by adjusting the torsion angles. The side chain of Trp227 was adjusted to avoid clashes with the aromatic rings of zopolrestat and minalrestat whereas torsion angles of Met120 and Phe311 were adjusted to avoid close contacts with all 3 inhibitors (Fig. 6).

All AKR1C21–inhibitor complexes were energy minimised to reduce steric hindrance using the Discover 2.7 package (Biosym Technologies Inc., San Diego, CA) on a Linux workstation. The constant valence force field incorporating the simple harmonic function for bond stretching and excluding all non-diagonal terms was used (cut off distance of 26 Å). Minimisation calculations were done using the algorithms steepest descents and conjugate gradients down to a maximum root mean square derivative of 10.0 kcal/Å and 0.01 kcal/Å, respectively. Molecular dynamics were then performed using leapfrog algorithms in Discover. Dynamics were equilibrated for 2 ps with times steps of 1 fs and then continued for 4 ps with time steps of 2 fs at 350 K. The resulting structure was extracted and energy minimised. This protocol allows some degree of conformational change to accommodate the inhibitor molecule in the active site and has been found to be effective for visualising the protein–ligand complex in a conformation close to its lowest energy structure.[48,49] Energy minimisation of the protein–inhibitor complexes resulted in a slight shift in the residues of the C-terminal loop, mimicking the conformational change it induces upon binding to AR. Figures were generated using *PyMOL* (DeLano Scientific, San Carlos, CA, USA) and MolScript.[50]

Acknowledgments

We thank Dr. Roland Chung for helpful suggestions during the preparation of the manuscript. This work was supported in part by an ARC Linkage International Award to O.E.K. and A.H. U.D. is the recipient of a MGS PhD Scholarship.

References and notes

1. Jez, J. M.; Penning, T. M. *Chem. Biol. Interact.* **2001**, *130–132*, 499–525.
2. Jez, J. M.; Bennett, M. J.; Schlegel, B. P.; Lewis, M.; Penning, T. M. *Biochem. J.* **1997**, *326*, 625–636.
3. Hyndman, D.; Bauman, D. R.; Heredia, V. V.; Penning, T. M. *Chem. Biol. Interact.* **2003**, *143–144*, 621–631.
4. Jez, J. M.; Flynn, T. G.; Penning, T. M. *Biochem. Pharmacol.* **1997**, *54*, 639–647.
5. Larson, E. R.; Lipinski, C. A.; Sarges, R. *Med. Res. Rev.* **1988**, *8*, 159–186.
6. Chung, S. S.; Chung, S. K. *Curr. Drug Targets* **2005**, *6*, 475–486.
7. Singh, S. B.; Malamas, M. S.; Hohman, T. C.; Nilakantan, R.; Carper, D. A.; Kitchen, D. *J. Med. Chem.* **2000**, *43*, 1062–1070.
8. Zenon, G. J., 3rd; Abobo, C. V.; Carter, B. L.; Ball, D. W. *Clin. Pharm.* **1990**, *9*, 446–457.
9. El-Kabbani, O.; Ruiz, F.; Darmanin, C.; Chung, R. P. *Cell. Mol. Life Sci.* **2004**, *61*, 750–762.
10. Hohman, T. C.; El-Kabbani, O.; Malamas, M. S.; Lai, K.; Putilina, T.; McGowan, M. H.; Wane, Y. Q.; Carper, D. A. *Eur. J. Biochem.* **1998**, *256*, 310–316.

11. Matsuda, H.; Morikawa, T.; Toguchida, I.; Yoshikawa, M. *Chem. Pharm. Bull. (Tokyo)* **2002**, *50*, 788–795.
12. Varma, S. D.; Mizuno, A.; Kinoshita, J. H. *Science* **1977**, *195*, 205–206.
13. Dostert, P.; Strolin Benedetti, M. *J. Pharmacol.* **1986**, *17*, 483–496.
14. Hamada, Y.; Nakamura, J. *Treat Endocrinol.* **2004**, *3*, 245–255.
15. Pfeifer, M. A.; Schumer, M. P.; Gelber, D. A. *Diabetes* **1997**, *46*, 82–89.
16. Sato, S.; Kador, P. F. *Biochem. Pharmacol.* **1990**, *40*, 1033–1042.
17. Vander Jagt, D. L.; Torres, J. E.; Hunsaker, L. A.; Deck, L. M.; Royer, R. E. *Adv. Exp. Med. Biol.* **1997**, *414*, 491–497.
18. El-Kabbani, O.; Carbone, V.; Darmanin, C.; Oka, M.; Mitschler, A.; Podjarny, A.; Schulze-Briese, C.; Chung, R. P. *J. Med. Chem.* **2005**, *48*, 5536–5542.
19. El-Kabbani, O.; Podjarny, A. *Cell. Mol. Life Sci.* **2007**, *64*, 1970–1978.
20. Lau, P. C.; Layne, D. S.; Williamson, D. G. *J. Biol. Chem.* **1982**, *257*, 9444–9449.
21. Lau, P. C.; Layne, D. S.; Williamson, D. G. *J. Biol. Chem.* **1982**, *257*, 9450–9456.
22. Nakagawa, M.; Tsukada, F.; Nakayama, T.; Matsuura, K.; Hara, A.; Sawada, H. *J. Biochem. (Tokyo)* **1989**, *106*, 633–638.
23. Ishikura, S.; Usami, N.; Nakajima, S.; Kameyama, A.; Shiraishi, H.; Carbone, V.; El-Kabbani, O.; Hara, A. *Biol. Pharm. Bull.* **2004**, *27*, 1939–1945.
24. Bellemare, V.; Faucher, F.; Breton, R.; Luu-The, V. *BMC Biochem.* **2005**, *6*, 12.
25. Bauman, D. R.; Steckelbroeck, S.; Penning, T. M. *Drug News Perspect* **2004**, *17*, 563–578.
26. Penning, T. M. *Hum. Reprod. Update* **2003**, *9*, 193–205.
27. Varma, S. D.; Kinoshita, J. H. *Biochem. Pharmacol.* **1976**, *25*, 2505–2513.
28. Urzhumtsev, A.; Tete-Favier, F.; Mitschler, A.; Barbanton, J.; Barth, P.; Urzhumtseva, L.; Biellmann, J. F.; Podjarny, A.; Moras, D. *Structure* **1997**, *5*, 601–612.
29. Darmanin, C.; Chevreux, G.; Potier, N.; Van Dorsselaer, A.; Hazemann, I.; Podjarny, A.; El-Kabbani, O. *Bioorg. Med. Chem.* **2004**, *12*, 3797–3806.
30. Soni, L. K.; Kaskhedikar, S. G. *Arch. Pharm. (Weinheim)* **2006**, *339*, 327–331.
31. Humber, L. G. *Prog. Med. Chem.* **1987**, *24*, 299–343.
32. Rastelli, G.; Ferrari, A. M.; Costantino, L.; Gamberini, M. C. *Bioorg. Med. Chem.* **2002**, *10*, 1437–1450.
33. Nakano, T.; Petrash, J. M. *Biochemistry* **1996**, *35*, 11196–11202.
34. Wilson, D. K.; Bohren, K. M.; Gabbay, K. H.; Quiocho, F. A. *Science* **1992**, *257*, 81–84.
35. Rondeau, J. M.; Tete-Favier, F.; Podjarny, A.; Reymann, J. M.; Barth, P.; Biellmann, J. F.; Moras, D. *Nature* **1992**, *355*, 469–472.
36. Borhani, D. W.; Harter, T. M.; Petrash, J. M. *J. Biol. Chem.* **1992**, *267*, 24841–24847.
37. Petrash, J. M.; Tarle, I.; Wilson, D. K.; Quiocho, F. A. *Diabetes* **1994**, *43*, 955–959.
38. Faucher, F.; Pereira de Jesus-Tran, K.; Cantin, L.; Luu-The, V.; Labrie, F.; Breton, R. *J. Mol. Biol.* **2006**, *364*, 747–763.
39. Dhagat, U.; Carbone, V.; Chung, R. P.; Schulze-Briese, C.; Endo, S.; Hara, A.; El-Kabbani, O. *Acta Crystallogr. Sect. F Struct. Biol. Cryst. Commun.* **2007**, *63*, 825–830.
40. Faucher, F.; Cantin, L.; Pereira de Jesus-Tran, K.; Lemieux, M.; Luu-The, V.; Labrie, F.; Breton, R. *J. Mol. Biol.* **2007**, *369*, 525–540.
41. Wilson, D. K.; Tarle, I.; Petrash, J. M.; Quiocho, F. A. *Proc. Natl. Acad. Sci. U.S.A.* **1993**, *90*, 9847–9851.
42. Steuber, H.; Zentgraf, M.; Gerlach, C.; Sotriffer, C. A.; Heine, A.; Klebe, G. *J. Mol. Biol.* **2006**, *363*, 174–187.
43. El-Kabbani, O.; Darmanin, C.; Schneider, T. R.; Hazemann, I.; Ruiz, F.; Oka, M.; Joachimiak, A.; Schulze-Briese, C.; Tomizaki, T.; Mitschler, A.; Podjarny, A. *Proteins* **2004**, *55*, 805–813.
44. Ehrig, T.; Bohren, K. M.; Prendergast, F. G.; Gabbay, K. H. *Biochemistry* **1994**, *33*, 7157–7165.
45. El-Kabbani, O.; Carper, D. A.; McGowan, M. H.; Devedjiev, Y.; Rees-Milton, K. J.; Flynn, T. G. *Proteins* **1997**, *29*, 186–192.
46. Barski, O. A.; Gabbay, K. H.; Bohren, K. M. *Biochemistry* **1996**, *35*, 14276–14280.
47. Podjarny, A.; Cachau, R. E.; Schneider, T.; Van Zandt, M.; Joachimiak, A. *Cell. Mol. Life Sci.* **2004**, *61*, 763–773.
48. Darmanin, C.; El-Kabbani, O. *Bioorg. Med. Chem. Lett.* **2000**, *10*, 1101–1104.
49. Darmanin, C.; El-Kabbani, O. *Bioorg. Med. Chem. Lett.* **2001**, *11*, 3133–3136.
50. Kraulis, P. *J. Appl. Crystallogr.* **1991**, *24*, 946–950.
51. Cornish-Bowden, A. In *Principles of Enzyme-Kinetics*, Butterworths: London, 1976, pp. 90–92.
52. Miyamoto, S. *Chem-Bio. Informatics J.* **2002**, *2*, 74–85.